invited paper submitted to JOSA B

# ELECTRIC FIELD POLING OF QUASI-PHASE-MATCHED OPTICAL FIBRES

390

P.G. Kazansky and V. Pruneri

Optoelectronics Research Centre,

University of Southampton,

Southampton SO17 1BJ,

United Kingdom

Tel +44 01703 593144

Fax +44 01703 593149

*Abstract*

Electric field poling of silica glass provides the prospect of efficient second-order nonlinear interactions in optical fibres. Recent advances in quasi-phase-matched second harmonic generation in electric field poled silica fibres are reviewed.

## I. Introduction

More than ten years have passed since the discovery of photoinduced quasi-phase-matched (QPM) second harmonic generation (SHG) in optical fibres [1-2]. However, until fairly recently, second harmonic generation in optical fibres has been more of scientific than practical interest, owing to the low levels of induced nonlinearity ( $\sim 10^{-3}$ pm/V, which is four orders of magnitude less than in inorganic crystals, e.g. lithium niobate) [3-17]. The mystery of photoinduced $\chi^{(2)}$ (second-order susceptibility) gratings was finally solved on the basis of the coherent photogalvanic effect [6]: a high ($10^{4-5}$ V/cm) spatially oscillating electrostatic field appears in glass as a result of charge separation induced by coherent photocurrent, oscillating with a period determined by the phase velocity mismatch between pump and second harmonic; this electric field produces a quasi-phase-matching (QPM) $\chi^{(2)}$ grating in proportion to $\chi^{(3)}$ (third-order susceptibility). The conversion efficiency reported in the first experiments on photoinduced SHG - $\sim 5\%$ from a peak pump power of $\sim 20$ kW - is still among the highest conversion efficiencies achieved so far in optical fibres (apart from the high fundamental peak intensity). The reasons for these relatively high conversion efficiencies has to be searched in the long length (tens of centimetres) and good uniformity of the photoinduced gratings.

During the past six years a number of glass poling techniques have emerged that produce second-order nonlinearities approaching 1 pm/V (very close to the value of nonlinearity in LBO, which is a crystal widely used for pulsed frequency conversion). These new poling techniques are: thermal poling at 250-300 °C under an applied electrical field (the second-

order nonlinearity appears in a thin layer just under the anode) [18], corona poling of glass waveguides [19] and charge implantation by exposure to an electron-beam [20]. To date the thermal poling technique has shown the most promising results in poling of silica fibres [21-23]. However a problem encountered in thermal poling is the spreading out of the poled regions caused by air breakdown that occurs when one attempts to create QPM $\chi^{(2)}$ gratings [22, 24]. Two solutions are possible to sidestep this problem: 1) electron beam or UV light can be used for selective erasure of uniformly poled sample [25]; 2) thermal poling in vacuo, using a patterned electrode, can create periodic $\chi^{(2)}$ patterns [26].

Continuous wave QPM frequency conversion to the blue has also been demonstrated in D-shaped optical fibres using patterned anodic electrode on the plane side, followed by thermal poling in vacuo. In out first work on frequency conversion to the blue at 430 nm [26], the maximum blue light power (in the $LP_{11}^{2\omega}$ second-harmonic (SH) mode) detected was $\sim 400$ pW, corresponding to a fundamental power in the fibre of $\sim 100$ mW. In a more recent work [27] we presented blue light generation at 440 nm, in the fundamental mode $LP_{01}^{2\omega}$, with an increase of a factor of ten in the conversion efficiency in comparison with the previous results. The interaction with the higher order SH modes was suppressed by side-etching of the fibre surface. We also tested uniformly poled fibres by using a tunable cw Ti:sapphire laser. Maker's oscillations of SH signal were observed corresponding to the value for the $\chi^{(2)}$ in the uniformly poled fibre of $\sim 1.4$ pm/V. When periodic poling was produced in the fibres the effective nonlinear coefficient $d_{eff}$ was $\sim$ 50 times smaller than the expected value of 0.22 pm/V ($=d/\pi$, $d=\chi^{(2)}/2$ ) for a periodic grating with an amplitude d of 0.7 pm/V, corresponding to the nonlinearity measured in the uniformly poled fibre. We believe

that this degradation was mainly due to the non uniformity of the grating (which was experimentally confirmed by direct optical image of the $\chi^{(2)}$ grating) although it is not excluded that the non-optimized overlap integral between interacting modes and poled region can still play a role in reducing the efficiency.

As we pointed out [26, 27], compared with polar crystals waveguides, such as lithium niobate (LN) and potassium titanyl phosphate (KTP), poled silica fibres offer greater bandwidths availability (more than one order of magnitude for the same device length) because of their lower dispersion. Therefore the relatively low value of the nonlinear coefficient could be compensated by increasing the length of the device, thus achieving the same efficiency as for LN and KTP without altering the frequency stability.

In the case of pulsed applications the group velocity mismatch (GVM) between pulses at different frequency determines the device length which should be the result of a good trade-off between high conversion efficiency and low pulse-spreading [28]. The low GVM in silica fibres (more than one order of magnitude less than in LN and KTP [29]), combined with the high optical damage threshold, makes poled silica a suitable material for pulsed frequency conversion since the relatively low nonlinear coefficient ($d_{eff}$) can be compensated by extended interaction lengths ($l_{eff}$) and high peak intensities ($I_p$), so that the figure of merit $d_{eff}^2 l_{eff}^2 I_p$ for the conversion efficiency is maintained high.

In this paper we review our recent results on QPM SHG in glasses. In the second section a brief theoretical background on QPM in periodically poled fibres is presented. In the third

section we report demonstration of efficient QPM SHG to the blue of picosecond pulses in a D-shape thermally poled fibre [30]. In the fourth section results on SHG in fibres poled via internal electrodes are presented. In the fifth section we discuss a new phenomenon - electrically stimulated growth of second-order nonlinearity grating in glass fibres.

## II. Theoretical background of quasi-phase-matched SHG in periodically poled fibre.

QPM second-order nonlinear optical interactions [31] ( e.g. SHG and parametric amplification) in periodically poled glass waveguides can be described using the general theory developed for modulated nonlinear crystal media (such as periodically poled ferroelectrics). The only difference is that, in the case of glass, the modulation for the nonlinear coefficient (d) is of the type +/0 (poled section alternated with unpoled section) rather than +/- as for ferroelectrics (domain reversal) (Fig.1). QPM occurs when the period $\Lambda$ for the modulation of the nonlinear coefficient d is a multiple integer of $2l_c$, where $l_c$ is the coherence length-distance over which fields and driving nonlinear polarizations undergo a $\pi$ phase-shift. In this way the unpoled sections allow periodic rephasing between the interacting fields without energy exchange, thus average compensation of the phase-mismatch. The final result in the case of the ideal square-like spatial modulation of d for first-order QPM is represented in fig.1, where a parabola-like spatial growth for the SH intensity is evident. In the same figure is shown also a non-phase-matched (NPM) interaction where d is not modulated (uniform poling) and the corresponding SH intensity oscillates without cumulative growth. What has been and will be said for QPM-SHG can be easily applied to any parametric interactions involving three waves in periodically poled glass.

The QPM waveguide condition establishes the dependence of the period Λ for the required modulation of d as a function of the fundamental wavelength and the typical waveguide parameters [24], i.e. for a fibre, core radius (a) and numerical aperture (NA):

$$\Lambda = \Lambda(\lambda,a,NA) = \frac{\lambda}{2[n_{eff}^{2\omega}(\lambda,a,NA) - n_{eff}^{\omega}(\lambda,a,NA)]}$$

where $n_{eff}^{\omega}$ and $n_{eff}^{2\omega}$ are the effective refractive indices at $\omega$ and $2\omega$ respectively.

An example of this dependence is shown in figs.2a, 2b for an interaction between fundamental modes ($LP_{01}$) at both $\omega$ and $2\omega$. The interaction could occur between modes of different orders. In particular, even in the case of single-mode silica fibre at the operating fundamental wavelength, the SH can develop in a higher order mode ($LP_{11}$, $LP_{21}$, $LP_{02}$, ...). Examples of the required grating period for QPM of several interactions between fundamental mode at $\omega$ and higher-order modes at $2\omega$ is shown in fig.3. From the curves it is clear that the QPM conditions allows, when necessary, selection of the generated SH mode.

In a QPM waveguide geometry and in a low fundamental depleted regime, the SH power $P_{2\omega}$ is given by:

$$P_{2\omega} = \frac{8\ \omega^2\ d_{eff}^{\ 2}}{n_{eff}(2\omega)\ n_{eff}^2(2\omega)\ \varepsilon_o\ c_o^3}\ \frac{P_\omega^{\ 2}}{A_{OVL}}\ \frac{1}{\Delta\beta^2}\ \sin^2\left(\frac{\Delta\beta\ L}{2}\right)\ \rho$$

where, apart from the already defined parameters, $P_\omega$ is the fundamental power, $d_{eff}$ is the nonlinear coefficient which includes the overlap between poled region and interacting modes as well as the $1/(m\pi)$ reduction factor associated with m-th order QPM, L is the device

length, $\varepsilon_o$ the dielectric constant in vacuum, $c_o$ the speed of light in vacuum, $A_{OVL}=1/I_{OVL}^2$ is an equivalent area which depends on the overlap $I_{OVL}$ between the interacting fields, $\Delta\beta = \Delta\beta(\omega) = 2(\omega/c_o)[\, n_{eff}(2\omega)-n_{eff}(\omega)]$ is the wave-vector mismatch and $\rho$ is an enhancement factor which takes account of the multimode nature of our fundamental source. As we will see in the following of this paper the optimization of the overlap between modes and the poled region constitute an important step toward significant efficiency. For example frequency doubling of 1.5 $\mu$m radiation is possible in a fibre single-mode both at the fundamental and SH wavelengths. However the efficiency would be reduced by the fact that the pump mode at 1.5 $\mu$m becomes very broad. Therefore it is more suitable to use a fibre not single mode at the SH wavelength and select the SH-$LP_{01}$ mode by making use of the appropriate QPM period (Fig.3).

The expression given for the SH power allows also to determine other crucial characteristics of the waveguide device. The acceptance QPM bandwidth (BW) can be defined as the full width at half maximum (in terms of wavelength, core radius, etc.) of the conversion efficiency curve ($sinc^2$ shape at low efficiency). It is evident, from the dependence of the wavelength bandwidth on the fundamental wavelength (Fig.4), the great bandwidth availability in silica fibres which in principle allows to use substantial long devices without compromising the frequency stability. In the same figure is also represented the corresponding group velocity mismatch (GVM) defined as the difference between the inverse of the group velocities at $\omega$ and $2\omega$ respectively:

$$GVM = GVM(\omega,a,NA) = \frac{1}{V_g(\omega,a,NA)} - \frac{1}{V_g(2\omega,a,NA)}$$

For a temporal pulse width $\tau$, the interacting pulses walk away over the typical distance $\tau$/GVM, which is usually called effective interaction length $l_{eff}$. The GVM prevents the quasi-quadratic cumulative growth and produces pulse broadening and pulse distortion. For these reasons $l_{eff}$ is a practical limit for the device length. One can appreciate the very low value of the GVM, making the periodically poled silica fibres very promising for pulsed applications (Fig.4) The curves for GVM and BW are consistent with the fact that the BW is inversely proportional to GVM in first order approximation, thus BW tends to diverge where GVM approaches zero (in fact BW is limited by higher order dispersion).

## III. Frequency doubling of picosecond pulses in periodically poled D-shape silica fibres

The D-shape fibre used in our experiments on SHG of short pulses [30] had a numerical aperture of 0.09, core and outer diameters of 5.8 and $\sim 150$ $\mu$m and distance between plane surface and core region of 5 $\mu$m. The poling technique was based on continuous voltage of $\sim 8$ kV applied via aluminium electrodes at $\sim 270$ °C for $\sim 10$ minutes in vacuo [26, 27]. The patterned aluminum electrode of 25 $\mu$m period was directly fabricated on the plane face of the D-shape fibre, rather than on a separate glass support which was afterwards pressed against the fibre. This allowed to realize more uniform gratings, $\sim 3$ times longer and with an increase of $\sim 5$ times in effective nonlinear coefficient, thus $>200$ times in conversion efficiency for the same fundamental intensity. To fabricate the patterned Al electrode (Fig.5), we initially placed the fibre on a planar substrate and then used ordinary photolithography. During poling the patterned electrode was the anode and the curved face of the fibre, in

contact with a metal substrate which was grounded, was the cathode. After poling the aluminum electrode was removed by etching. The length of the grating was chosen to be $\sim 1.8$ cm which is close to the ratio $\tau$/GVM at around 840 nm, between the pulse duration $\tau$ of $\sim 2.2$ ps and the GVM of $\sim 0.14$ ps/mm. This ratio is the length over which the walk-off of the interacting pulses takes place and gives a good conversion efficiency without significant pulse lengthening.

Before carrying out the picosecond experiment we optically assessed the sample using a tunable Ti:sapphire laser as fundamental source. The quasi-phase-matching curve (SH power against fundamental wavelength) is shown in fig.6. The bandwidth (FWHM) of $\sim 0.42$nm agrees well with the calculated value for a perfect nonlinear periodic structure of the same length indicating the good uniformity of the grating over the whole length. From fig.6 it is also evident the presence of much weaker interaction with higher order SH modes ($LP_{11}^{2\omega}$, $LP_{21}^{2\omega}$) at shorter wavelengths. The maximum cw blue power produced at 422.3 nm was $\sim 1.1$ mW corresponding to a fundamental power of 150 mW. From these measurements one can easily calculate an effective nonlinear coefficient of $\sim 1.5 \cdot 10^{-2}$ pm/V(which includes the overlap of the modes with the poled region and the $1/\pi$ reduction factor associated with first-order QPM). This value is still more than 10 times lower than the limit of $\sim 2.2 \cdot 10^{-1}$ pm/V that we have estimated from measurements on uniformly poled silica fibres [27]. The reasons of this degradation are probably the spreading of the poled regions, which produce mark-to-space ratio far from the optimum 50/50 and lower depth of nonlinear modulation, as well as the presence of regions completely poled or unpolled rather than periodically poled.

For the pulsed experiment the fundamental source was a tunable mode-locked Ti:sapphire laser which produced $\sim 2.2$ ps pulses at a repetition rate of 76 MHz. The maximum average SH power was $\sim 76$ mW corresponding to an average fundamental power of 35 mW ($\sim 200$ W peak power) at wavelength of 844.6 nm. Therefore the maximum conversion efficiency was $\sim 0.22$ % which corresponds to a normalized conversion efficiency with respect to the average fundamental power of $\sim 6.3$ %/W.

## IV. Second-harmonic generation in fibres poled via internal electrodes under UV and thermal excitation

Fibre with in-built capillaries on either side of the core, suitable for introducing wire electrodes [32], are very attractive for poling techniques. Fujiwara et al [33] recently reported an electrooptic coefficient as high as 6 pm/V in these fibres, poled under UV excitation. The applied electric field was only 80 V/$\mu$m (800 V across gap of 10 $\mu$m) in these experiments - not sufficient to produce any significant electric field-induced second-order nonlinearity via the third-order nonlinearity. It is possible that phenomena other than the Pockel's effect contribute to the high value of coefficient obtained. These phenomena, if they exist, are unlikely to play a role in SHG.

In our experiments we used Ge-doped silica fibres with built-in capillaries on both sides of the core, suitable for introducing wire electrodes (Fig.7). A typical fibre used in our experiments had 0.32 numerical aperture, 3 $\mu$m core diameter, 165 $\mu$m outer diameter, 50 $\mu$m hole diameter and 9 $\mu$m interhole spacing. Metal wires of 25 $\mu$m diameter were inserted

into the fibre over length varying from 5 mm to 500 mm.

The first fibres were poled for 30 min with $\sim 1$ kV applied voltage and simultaneous excitation with 193 nm laser pulses from an ArF excimer laser at an energy density of $\sim 100$ mJ/cm$^2$. We also poled fibres at $\sim 1$ kV for 45 min without any UV irradiation. Only weak SH signals, corresponding to $\chi^{(2)}$ less than 0.02 pm/V, were observed.

We also thermally poled fibres using two internal electrodes, and one internal and one external electrode, applying a voltage in the range 5 kV to 9 kV. First we used a mode-locked (76 MHz repetition rate, 300 ps pulse duration) and Q-switched (1 kHz repetition rate, 300 ns envelope duration) Nd-YAG laser operating at 1064 to test these fibres. Oscillations of the SH signal generated in higher order modes were observed when the temperature was tuned from 20°C to 80°C. These SH oscillations resembled Mayker's oscillations of non phase-matched SH signal. We measured conversion efficiencies of 0.14% at a peak pump power of $\sim 1.7$ kW. However when we pumped with a tunable cw Ti:sapphire laser several broad (about 30 nm) regions with similar oscillations of the SH signal generated in higher-order modes (see fig.8), separated by regions where the SH signal was almost absent, were observed. The latter observation led us to the conclusion that the SH oscillations with the temperature as well as with the wavelength we detected are related to modal phase-matching. The value of $\chi^{(2)}$ in these fibres is still unclear due to uncertainty in the coherence length and overlap integral for the nonlinear interactions when higher order SH modes are involved.

## V. Electrically stimulated growth of $\chi^{(2)}$ gratings in silica fibres

During our experiments on fibres with internal electrodes we observed a new physical phenomenon which was named the electrically induced growth of $\chi^{(2)}$ gratings [34]. It has been known since the discovery of photoinduced SH generation in optical fibres, that when a sample of glass or glass fibre (e.g. Ge-doped silica fibre) is illuminated for some time (preparation time) with intense light containing frequencies at $\omega$ (pump) and $2\omega$ (second harmonic seeding) and afterwards the seeding is removed, it is still possible to observe light at frequency $2\omega$ (second harmonic) generated in the glass [1-2]. In experiments on optical glass fibres strong amplification of a weak seeding radiation at frequency $2\omega$, generated inside a fibre as a result of magnetic dipole or quadrupole effects, is observed after launching only intense light at frequency $\omega$ (without external seeding) [1-2].

Firstly, during our experiments, we launched only infrared light (pump) of $\sim 12$ mW average power (1 kW peak power) for $\sim 1$ hour into the fibre, $\sim 25$ cm long. A mode-locked and Q-switched Nd-YAG laser operating at 1064 nm was used as the pump source. No SH generation was observed in the fibre. Then we launched simultaneously the pump of $\sim 12$ mW average power and the SH seeding of $\sim 40$ $\mu$W average power, generated in a KTP crystal. The SH seeding was removed after preparation of $\sim 10$ min and a SH signal of $\sim 20$ $\mu$W average power was observed, corresponding to a conversion efficiency of $\sim 0.16\%$. This was confirmed by monitoring the growth of the SH signal in the fibre when the SH seeding was blocked for a short time during the preparation (Fig.9). Our result is in good agreement with previous observations on photoinduced SHG in Ge-doped fibres [1-2] and may be explained by the appearance of a modulated second-order nonlinearity ($\chi^{(2)}$ grating) in the fibre.

We then applied high voltages up to 10 kV (corresponding to electrical fields $\sim 10^7$ V/cm, which are probably among the highest values ever applied to glass materials) across the electrodes inside the fibre and launched into the fibre (25 cm long) IR pump light of $\sim 1$ kW peak power. The length of the region over which the electric field had been applied (electrode superposition) was $\sim 20$ cm long. For applied voltages greater than $\sim 2$ kV a strong increase of a weak electric-field induced second harmonic (EFISH) signal of $\sim 10$ nW (i.e. generated immediately after the electric field was applied) was observed (Fig.9). In fact the SH signal grows rapidly, within 1 min time-scale, reaching the maximum value of $\sim 250$ $\mu$W average power and then slowly decreases (Fig.9). After this first growth and decrease an interesting "echo" behaviour was observed when the voltage was repeatedly switched off and on (Fig.10). After disconnecting the voltage, the SH signal rapidly drops, remaining zero for a short time period, then increases, reaching almost 60% of the maximum value when the voltage was applied and finally slowly decreases again (Fig.10). During these experiments we achieved conversion efficiencies as high as $\sim 2\%$ for a peak pump power of $\sim 1$ kW, which is $\sim 10$ times higher than in our experiments carried out without applying an external electric field. We detected $\sim 4$ times smaller SH signal and $\sim 2$ smaller growth rate in a fibre with electrode superposition $\sim$ 10 cm long, thus two times shorter than in the previous fibre used.

We excluded a simple explanation of this phenomenon by the EFISH seeding of $\chi^{(2)}$ grating in a fibre on the basis of two experimental observations. Firstly, we observed that the second harmonic growth took place only in the region where the electric field was applied (where the electrodes superposed) and the SH output was quadratic dependent on the length of this region. Secondly, no SHG signal was observed in any of the used fibres after preparation for more than 1 hour with a weak external SH seeding of the same and even an order of magnitude higher level of power compared to the EFISH maximum signal. The maximum

SH signal (Fig.11a) and time, necessary to reach half of the maximum (Fig.11b), when the voltage is switched-on and switched-off, clearly depend on the applied voltage: the maximum SH signal increases with the applied voltage whereas the half-growth time decreases with the applied voltage.

The high conversion efficiency measured in our experiments and the observed quadratic dependence of the SHG efficiency on the fibre length represent clear evidences of quasi-phase-matched SHG due to presence of a $\chi^{(2)}$ grating in the fibre. Moreover the enhancement of SHG in glass due to a strong applied electric field ($\sim 5 \times 10^6$ V/cm) was confirmed by experimental observation that the amplitude of the $\chi^{(2)}$ grating increases at least $\sim 3$ times (corresponding to an increase of conversion efficiency $\sim 10$ times) compared to experimental situations where no electric field is applied to the fibre.

Our experimental results can be explained as follows. Firstly we would like to remind that the explanation for the phenomenon of photoinduced second harmonic generation is based on the coherent photocurrent, excited in glass as a result of interference between one-photon ionization by light at frequency $2\omega$ and two-photon ionization by light at frequency $\omega$ [6]. Indeed, the probability P of simultaneous ionization of defect site by two photons at frequency $\omega$ and one photon at frequency $2\omega$ is given by:

$$P \sim |a_2 E_\omega E_\omega + a_1 E_{2\omega}|^2 = |a_2|^2 I_\omega^2 + |a_1|^2 I_{2\omega} + 2\mathrm{Re}\{a_1^* a_2 E_\omega E_\omega E_{2\omega}^*\} \qquad (1)$$

where $E_\omega$ and $E_{2\omega}$ are the fields amplitudes at frequency $\omega$ and $2\omega$ respectively, $I_\omega$ and $I_{2\omega}$ are the corresponding intensities and $a_1$ and $a_2$ are two complex coefficients which determine the weight of the different processes in the probability P. The first two terms, proportional to even powers of the electric fields, describe the photoconductivity $\sigma$:

$$\sigma \sim |a_2|^2 I_\omega^2 + |a_1|^2 I_{2\omega}$$

and the last term, proportional to odd power of the fields, describes the coherent

photocurrent $j_{coh}$ or the modulation for the angular distribution of photoelectrons:

$j_{coh} \sim 2Re\{a_1^* a_2 E_\omega E_\omega E_{2\omega}^*\}$

Therefore the coherent photocurrent spatially oscillates with a period $\Lambda$ determined by the refractive index mismatch between light waves at frequencies $\omega$ and $2\omega$:

$j_{coh} \sim \cos 2\pi z/\Lambda, \qquad \Lambda = \lambda/2(n_{2\omega} - n_\omega),$

where $\lambda$ is the wavelength in vacuum of the light at frequency $\omega$, $n_{2\omega}$ and $n_\omega$ are the refractive indices at frequencies $2\omega$ and $\omega$ respectively. This photocurrent gives rise to an electrostatic (dc) field $E_g$ (photogalvanic field): $E_g \simeq j_{coh}/\sigma$. The magnitude of the photogalvanic field $E_g$ in glass is typically $\sim 10^4$-$10^5$ V/cm and this field can induce a modulation in the second order nonlinear susceptibility ($\chi^{(2)}$) via the third-order nonlinearity:

$\chi^{(2)} = 3\chi^{(3)} E_g \sim \cos 2\pi z/\Lambda$. Assuming $\chi^{(3)} \simeq 10^{-22}$ $(m/V)^2$ for silica glass, the amplitude of $\chi^{(2)}$ is $\sim 10^{16}$-$10^{15}$ m/V. It turns out that the $\chi^{(2)}$ periodicity can compensate for the phase velocity mismatch (refractive index mismatch), thus making the second harmonic process efficient.

The coefficients $a_1$ and $a_2$ in the expression of the probability P can depend on the pump and second harmonic intensities: $a_1 = a_1(I_\omega^2, I_\omega^3, I_{2\omega})$, $a_2 = a_2(I_\omega^2, I_\omega^3, I_{2\omega})$. The physical interpretation of such dependence consists in the following: the ground level of the defect site in the one- and two-photon ionizing transitions can be populated from other defect levels, lower in energy and more densely populated. The last transition could be produced by one-photon ($2\omega$ photon or $3\omega$ photon, generated as a result of the third harmonic generation) or two-photon ($\omega + \omega$ or $\omega + 2\omega$) absorptions.

It is possible to interpret the coherent photocurrent in glass in terms of electronic wave-functions interference [35]. Indeed, in centrosymmetric media one-photon transition is allowed between states of different parity and two-photon transition between states of the

same parity. If the ground state for one- and two-photon transitions is the same, then the parity of the corresponding excited states should be different. The interference of electronic wave- functions of different parity in the continuum of states (conduction band) results in asymmetric wavefunction, leading to photocurrent. The orthogonality of the wave-functions in the excited state of the one-and two-photon transitions in centrosymmetric media leads also to the absence of modulation of the total cross section of ionization (coherent photoconductivity) in this process.

Let us now consider interaction of light beams of frequencies $\omega$ and $2\omega$ in glass when a strong dc electric field ( $E_o >> E_g$ ) is applied. The probability of simultaneous ionization of defect site by two photons at frequency $\omega$ and one photon at frequency $2\omega$ in the presence of $E_o$ is given by:

$$P \sim |a_2 E_\omega E_\omega + b_2 E_o E_{2\omega}|^2 = |a_2|^2 I_\omega^2 + |b_2|^2 I_{2\omega} E_o^2 + 2\mathrm{Re}\{a_2 b_2^* E_o E_\omega E_\omega E_{2\omega}^*\} \qquad (2)$$

where the symbols used have the same meaning as for equation (1). All terms in this expression are even powers of the electric field regardless they are uniform (first two terms) or modulated (being dependent on the relative phase of the fields at frequencies $\omega$ and $2\omega$ (the last term)). Unlike in the process without dc electric field considered above, the modulated part of the probability leads to modulation of the total ionization cross section and hence to a corresponding modulation of the photoconductivity:

$$\sigma = \sigma_o + \sigma_{coh},$$

where

$$\sigma_o \sim |a_2|^2 I_\omega^2 + |b_2|^2 I_{2\omega} E_o^2$$

is the uniform part of the photoconductivity and

$$\sigma_{coh} \sim 2\mathrm{Re}\{a_2 b_2^* E_o E_\omega E_\omega E_{2\omega}^*\} \sim \cos 2\pi z/\Lambda$$

is the part of the photoconductivity being dependent on the relative phase between $E_\omega$ and $E_{2\omega}$ (coherent photoconductivity).

The ohmic current ( $j = \sigma E_o$) induced by the applied electric field separates photocarries which accumulate at the boundaries of the illuminated region and screen the applied electric field $E_o$. The resulting internal electric field inside the glass $E_c$ evolves accordingly to:

$dE_c/dt = -E_c/\tau$, $\tau = \epsilon/\sigma$,

where $\tau$ is the dielectric relaxation time and $\epsilon$ is dielectric constant of glass. An approximate solution for $E_c$ in the limit $\sigma_{coh} << \sigma_o$ , $\tau = \tau_o = \epsilon/\sigma_o$ is:

$$E_c \simeq \sigma_{coh}/\sigma_o \, E_o\{1 - \exp(-t/\tau_o)\}\exp(-t/\tau_o) + E_o\exp(-t/\tau_o) =$$

$$= E_c^{coh} + E_c^{o}, \qquad (3)$$

where $E_c^{coh}$ and $E_c^{o}$ are the modulated and uniform part of the internal electric field. The modulated part of the electric field, proportional to $\sigma_{coh}$, and the corresponding $\chi^{(2)} = 3\chi^{(3)} E_c^{coh}$ are zero at the beginning (t=0), reach maximum values at $t = \tau_o \ln 2$ and finally decreases to zero in the steady state condition ($t=\infty$).

It should be noted that no modulation of the angular distribution of photoelectrons takes place in a process, such as the above interference, where one- and two-photon ionizing transitions in a strong dc electric field ($E_o >> E_g$) are involved.

Our experimental results can be qualitatively interpreted in the light of the mechanism presented above, i. e. on the basis of photoconductivity being dependent on the relative phase between interacting waves at frequencies $\omega$ and $2\omega$, which provides quasi-phase-matching for the SH generation. From our measurements we can also estimate the amplitude of the second-order susceptibility $\chi^{(2)} \simeq 10^{-14}$ m/V, which corresponds to a modulation of $\sim 8\%$ in the applied electric field. More important this model is consistent with the increase in conversion efficiency with the applied voltage and is also in good agreement with the experimental time dependence of the SH signal growth to a maximum value followed by a gradual decay. Moreover, an interesting feature in the time dependence of the SH signal -

the origin of an unexpected growth ("echo") of the SH signal after switching-off the voltage (Fig.10) - can be explained. Indeed, as follows from equation (3) in steady state conditions the internal electric field $E_c$ is zero, which means that the applied dc electric field $\mathbf{E}_0$ is locally compensated by the electric field $\mathbf{E}_s$ due to the screening charges, accumulated at the boundaries of the illuminated region: $\mathbf{E}_c = \mathbf{E}_0 + \mathbf{E}_s \simeq 0$, $\mathbf{E}_0 \simeq -\mathbf{E}_s$. After switching-off the voltage ($E_0 = 0$) the internal electric field rapidly increases almost to its initial value $\mathbf{E}_c \simeq \mathbf{E}_s \simeq -\mathbf{E}_0$. This rapid increase induces in the glass an index change due to Kerr effect, thus a phase mismatch between pump, SH waves and a remaining weak $\chi^{(2)}$ grating. Initially, the SH signal quickly drops to zero as a result of this phase-mismatch. However due to the fact that the internal electric field increases almost to its initial value (with opposite polarity), the process of electrically stimulated growth of $\chi^{(2)}$ grating via coherent phoconductivity repeats itself for a second time.

## VI. Conclusions

In conclusion, our results show that periodically poled silica fibres have become a promising medium for second-order nonlinear frequency conversion. In particular, D-shape silica fibres have been periodically poled at elevated temperature by applying high voltage via a patterned electrode deposited on the plane face. The resulting nonlinear grating of 25 $\mu$m period, uniform over the whole 1.8 cm length, has been used for quasi-phase-matched second harmonic generation. With a mode-locked laser as fundamental source blue powers up to ~76 mW have been generated at ~422 nm with an average conversion efficiency of ~0.22%. Considering that the effective nonlinear coefficient can still improve >10 times (corresponding potential increase in conversion efficiency >100), great progress is expected from optimization of the poling conditions.

We have observed electrically stimulated light-induced second harmonic generation in glass due to periodic modulation of a strong applied electrostatic field induced by light at frequencies $\omega$ and $2\omega$. During these experiments we achieved conversion efficiencies as high as ~2% for a peak pump power of ~1 kW, which is ~10 times higher than in our experiments carried out without applying an external electric field. It should also be mentioned that the interference between different quantum processes, which constitute the basics of this phenomenon, has been the subject of considerable attention in many areas of physics [35-41]. One of the reasons for this growing interest is that such a kind of interference open a prospect of a new degree of freedom in the control of physical processes - not only by the intensity or the polarization of light, but also by the phase of light. In the phenomenon of *efficient* SH generation in glass subjected to a strong external electrostatic field, the spatial periodic modulation of the applied electric field, responsible for the second harmonic signal, arises from the interaction of the intense light at frequencies $\omega$ and $2\omega$ with glass, which has its inversion symmetry broken by the applied field. The process could represent the first evidence of photoconductivity being dependent on the relative phase between light waves of different frequencies.

The search of new glass-based materials with high second-order nonlinearities can lead to discovery of new $\chi^{(2)}$ materials with advanced properties. Recently, we identified new nonlinear crystals - Ga:La:S and $\alpha$-$Ga_2S_3$ - as responsible for the frequency doubling process in Ga:La:S based glasses [42]. Fabrication of glasses with periodically oriented micro- or nanocrystals could provide an attractive way of achieving efficient quasi-phase-matched parametric interactions.

## References


1. U. Österberg and W. Margulis, "Dye laser pumped by Nd:YAG laser pulses frequency doubled in glass optical fibre," Opt. Lett. **11**, 516 (1986).
2. R.H. Stolen and H.W.K. Tom, "Self-organized harmonic generation in optical fibres," Opt. Lett., **12**, 585 (1987).
3. N.B. Baranova and B.Ya. Zeldovich, "Extension of holography to multiwavelength fields," JETP Lett., **45**, 716 (1987).
4. M.C. Farries, P.St.J. Russell, M.E. Fermann and D.N. Payne, "Second harmonic generation in an optical fibre by self-written $\chi^{(2)}$ grating," Electron. Lett., **23**, 322 (1987).
5. V. Mizrahi, U. Osterberg, C. Krautchik, G.E. Stegeman, J.E. Sipe and T.P. Morse, "Direct test of a model of efficient second-harmonic generation in optical fibres, " Appl. Phys. Lett., **53**, 557 (1988).
6. E.M. Dianov, P.G. Kazansky and D.Yu. Stepanov, "Problem of the photoinduced second harmonic generation," Sov. J. Quantum. Electron., **19**, 575 (1989); "Photovoltaic model of photoinduced second harmonic generation in optical fibres," Sov. Lightwave Commun., **1**, 247 (1991); E.M. Dianov, P.G. Kazansky, D.S. Starodubov and D. Yu. Stepanov, "Photoinduced second harmonic generation: observation of charge separation due to the photovoltaic effect," Sov. Lightwave Commun., **3**, 83 (1992).
7. F. Ouellette, K. Hill and D.C. Johnson, "Enhancement of second-harmonic generation in optical fibres by hydrogen and heat treatment," Appl. Phys. Lett., **54**, 1086 (1989).
8. R. Kashyap, "Phase-matched periodic electric-field-induced second-harmonic generation in optical fibres," J. Opt. Soc. Am. **B 6,** 313 (1989).

9. L. Li and D.N. Payne, "Permanently-induced linear electro-optic effect in silica optical fibres," in Digest of Conference on Integrated and Guided Wave Optics (Optical Society of America, Washington, D.C., 1989), paper TuAA2-1.

10. V. Mizrahi, Y. Hibino and G. Stegeman, "Polarization study of photoinduced second-harmonic generation in glass optical fibres," Opt. Commun., **78**, 283 (1990).

11. A. Kamal, D.A. Weinberger and W.H. Weber, "Spatially resolved Raman study of self-organized $\chi^{(2)}$ gratings in optical fibres," Opt. Lett., **15**, 613 (1990).

12. M.D. Selker and N.M. Lawandy, "Observation of seeded second-harmonic generation in bulk germanosilicate fibre," Opt. Commun. **77**, 339 (1991).

13. D. Anderson, V. Mizrahi and J.E. Sipe, "Model for second-harmonic generation in glass optical fibres based on asymmetric photoelectron emission from defect sites," Opt. Lett., **16**, 796 (1991).

14. F. Charra, F. Devaux, J.M. Nunzi and P. Raimond, "Picosecond light-induced noncentrosymmetry in dye solution," Phys. Rev. Lett., **68**, 2440 (1992).

15. V. Dominic and J. Feinberg, "Growth rate of second-harmonic generation in glass," Opt. Lett., **17**, 1761 (1992).

16. D.M. Krol, D.J. DiGiovanni, W. Pleibel and R.H. Stolen, "Observation of resonant enhancement of photoinduced second-harmonic generation in Tm-doped aluminosilicate glass fibres," Opt. Lett., **18**, 1220 (1993).

17. W. Margulis, F. Laurell, B. Lesche, "Imaging the nonlinear grating in frequency-doubling fibres," Nature, **378**, 649 (1995).

18. R.A. Myers, N. Mukherjee and S.R.J. Brueck, "Large second-order nonlinearities in poled fused silica," Opt. Lett. **16**, 1732 (1991).

19. A. Okada, K. Ishii, K. Mito and K. Sasaki, "Second-harmonic generation in novel corona poled glass waveguides," Appl. Phys. Lett. **60**, 2853 (1992).

20. P.G. Kazansky, A. Kamal and P.St.J. Russell, "High second-order nonlinearities induced in lead silicate glass by electron-beam irradiation," Opt. Lett. **18**, 693 (1993).

21. P.G. Kazansky, L. Dong and P.St.J. Russell, "High second-order nonlinearities in poled silicate fibres," Opt.Lett., **19**, 701 (1994).

22. P.G. Kazansky, L. Dong and P.St.J. Russell, "Vacuum poling: an improved technique for effective thermal poling of silica glass and germanosilicate optical fibres," Electron. Lett., **30**, 1345 (1994).

23. X.-C. Long, R.A. Myers and S.R.J. Brueck, "A poled electrooptic fibre," IEEE Photon. Tech. Lett., **8**, 227 (1996).

24. R. Kashyap, G.J. Veldhuis, D.C. Rogers and P.F. McKee, "Phase-matched second-harmonic generation by periodic poling of fused silica," Appl. Phys. Lett., **64**, 1332 (1994).

25. P.G. Kazansky, A. Kamal and P.St.J. Russell, "Erasure of thermally poled second-order nonlinearity in fused silica by electron implantation," Opt. Lett. **18**, 1141 (1993).

26. P.G. Kazansky, V. Pruneri and P.St.J. Russell, "Blue-light generation by quasi-phase-matched frequency doubling in thermally poled optical fibres," Opt. Lett., **20**, 843, (1995).

27. V. Pruneri and P.G. Kazansky, "Electric-field thermally poled optical fibres for quasi-phase-matched second harmonic generation," IEEE Photon. Tech. Lett., **6**, N2 (1997).

28. K. Hayata, and M. Koshiba, "Group-velocity-matched second-harmonic generation: An efficient scheme for femtosecond ultraviolet pulse generation in periodically domain-inverted b-$BaB_2O_4$," Appl. Phys. Lett., **62**, 2188 (1993).

29. V. Pruneri, S.D. Butterworth, and D.C. Hanna, "Highly efficient green-light

generation by quasi-phase-matched frequency doubling of picosecond pulses from an amplified mode-locked Nd:YLF laser," Opt. Lett., **21**, 390 (1996).

30. V. Pruneri and P.G. Kazansky, "Frequency doubling of picosecond pulses in periodically poled D-shaped silica fibre," to be published in Electron. Lett.

31. J.A. Armstrong, N. Bloembergen, J. Ducuing and P.S. Pershan, "Interaction between light waves in a nonlinear dielectric," Phys. Rev. **127**, 1918 (1962).

32. M.-V. Bergot, M.C. Farries, M.E. Fermann, L. Li, L.J. Poyntz-Wright, P.St.J. Russell and A. Smithson, "Generation of permanent optically-induced 2nd order nonlinearities in optical fibres by poling," Opt. Lett. **13**, 592 (1988).

33. T. Fujiwara, D. Wong,Y. Zhao, S. Fleming, S. Poole and M. Sceats, "Electro-optic modulation in germanosilicate fibre with UV-excited poling," Electron. Lett., **31**, 573 (1995).

34. P.G. Kazansky and V. Pruneri, "Electrically stimulated light-induced second-harmonic generation in glass: evidence of coherent photoconductivity," submitted (1997).

35. E. Dupont, P. B. Corkum, H. C. Liu, M. Buchanan, and Z. R. Wasilevski, "Phase-controlled currents in semiconductors," Phys. Rev. Lett. **74**, 3596 (1995).

36. Y.Y. Yin, C. Chen, D.S. Elliot, and A.V. Smith, "Asymmetric photoelectron angular distribution from interfering photoionization processes," Phys. Rev. Lett. **64**, 2353 (1992).

37. N.B. Baranova, A.N. Chudinov, A.A. Shulginov, and B.Ya. Zel'dovich, "Polarization dependence of the phase of interference between single- and two-photon ionization," Opt. Lett. **16**, 1346 (1991).

38. J. C. Miller, R. N. Compton, M. G. Payne, and W. R. Garrett, "Resonantly enhanced multiphoton ionization and third harmonic generation in xenon gas,"

Phys. Rev. Lett. **45**, 114 (1980).

39. S. M. Park, S. P. Lu, and R. J. Gordon, "Coherent laser control of the resonance-enhanced multiphoton ionization of HCl," J. Chem. Phys. **94**, 8622 (1991).

40. C. Chen, Y. Y. Yin, and D. S. Elliot, "Interference between optical transitions," Phys. Rev. Lett. **64**, 507 (1990).

41. R. J. Glauber, "Coherence and quantum detection," in *Quantum Optics* edited by R. J. Glauber, Proceedings of the E. Fermi International School in Physics, Vol. 62 ( New York - London: Acad. Press, 1969).

42. V. Pruneri, P.G. Kazansky, D. Hewak, J. Wang, H. Takebe and D. Payne, "Frequency doubling in gallium-lanthanum-sulphide optical glass with microcrystals," Appl. Phys. Lett., **70**, 155 (1997).

***Figure captions***

Fig.1 First-order QPM. The nonlinear coefficient d is modulated over a period equal twice the coherence length ($l_c$ ) by periodic alternation of poled and unpolled section. The step growth for the SH intensity is quasi-quadratic (solid line). The non-phase-matched case is also shown (dashed line).

Fig.2 QPM grating period as a function of fundamental wavelength for different core radius (a), and as a function of core radius for different wavelengths (b) in a silica fibre. The modes are fundamental ($LP_{01}$) at both $\omega$ and $2\omega$. The NA of the fibre is 0.17 which provides cut-off wavelengths (indicated with filled circle) of 1.15, 1.33, 1.51 $\mu$m for core radius of 2.6, 3, 3.4 $\mu$m respectively.

Fig.3 QPM grating period as a function of the fundamental wavelength for different interactions in a silica fibre. The NA of the fibre is 0.17 and the core radius 3 $\mu$m.

Fig.4 Group velocity mismatch and acceptance bandwidth for QPM-SHG as functions of the fundamental wavelength in a silica fibre with NA=0.17.

Fig.5 Aluminium pattern (25 $\mu$m period and 1.8 cm long) on the plane face of the D-shape fibre.

Fig.6 Quasi-phase-matching curve: SH power against fundamental wavelength.

Fig.7 Cross-section of a Ge-doped silica fibre with internal electrodes. The fibre had 0.32 numerical aperture, 3 μm core diameter, 165 μm outer diameter, 50 μm hole diameter and 9 μm interhole spacing. Metal wires of 25 μm diameter were inserted into the fibre over length varying from 5 mm to 500 mm.

Fig.8 SH power versus fundametal wavelength in a fibre thermally poled via internal electrodes.

Fig.9 Time dependence of SH signal in a fibre with external SH seeding of ~40 μW average power (opened triangles). The seeding was launched at t =0. The SH growth was monitored by blocking the SH seeding. Time dependence of SH signal in a fibre with applied voltage of 5 kV (filled triangles). The voltage was switched on at t = 0. The length of the fibre is ~25 cm and the superposition of the electrodes is ~ 20 cm. Average pump power is ~12 mW.

Fig.10 Time dependence of SH signal in a fibre when an applied voltage of 5 kV was repeatedly switched on and off. The instants when the voltage is on and off are shown by arrows.

Fig.11 Dependencies of the maximum SH signal (a) and the time necessary for reaching half of this maximum (b) on applied voltage when the voltage is switched ON and OFF respectively.

P.G. Kazansky and V. Pruneri "Electric field poling of quasi-phase-matched optical fibres", Fig.1

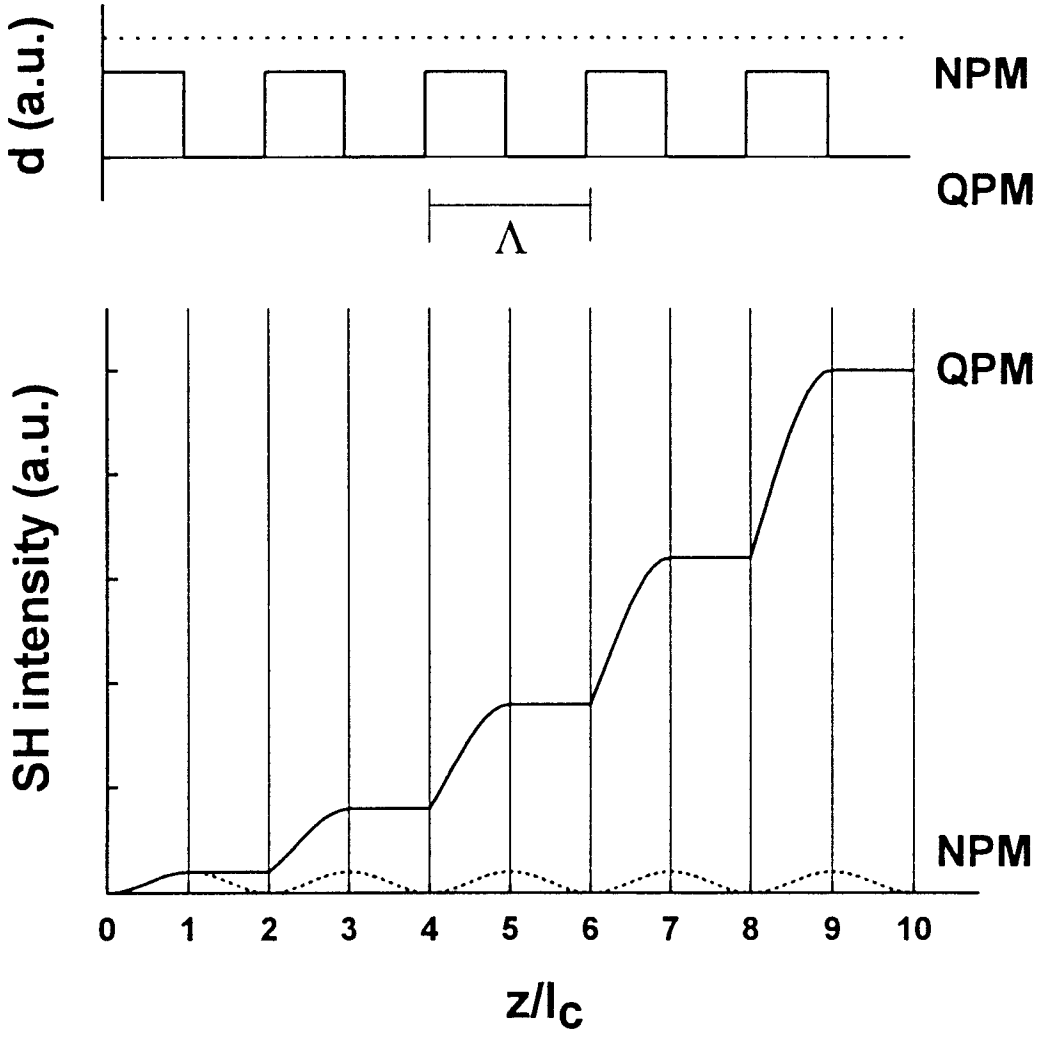

P.G. Kazansky and V. Pruneri "Electric field poling of quasi-phase-matched optical fibres", Fig.2a

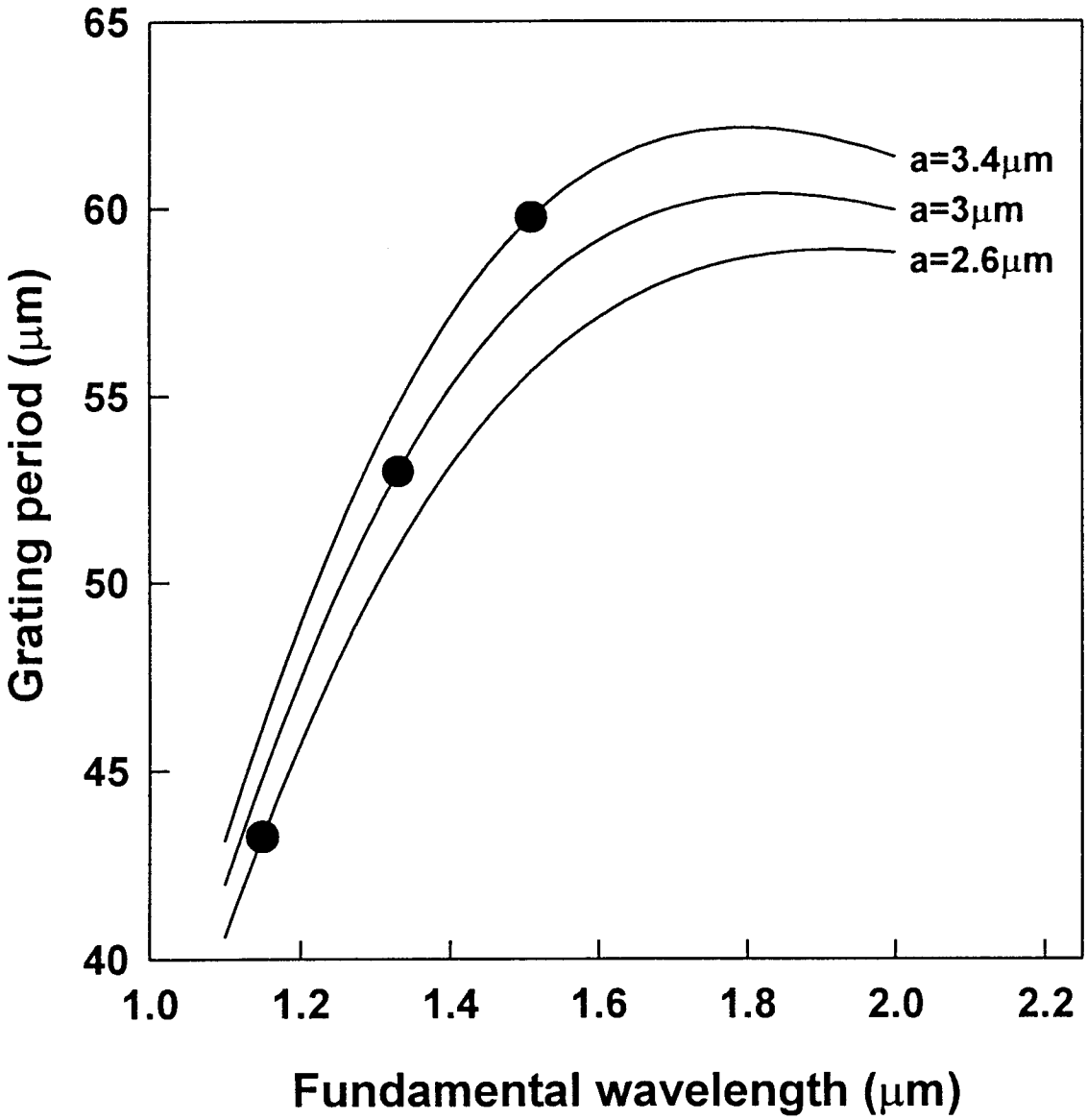

P.G. Kazansky and V. Pruneri "Electric field poling of quasi-phase-matched optical fibres", Fig.3

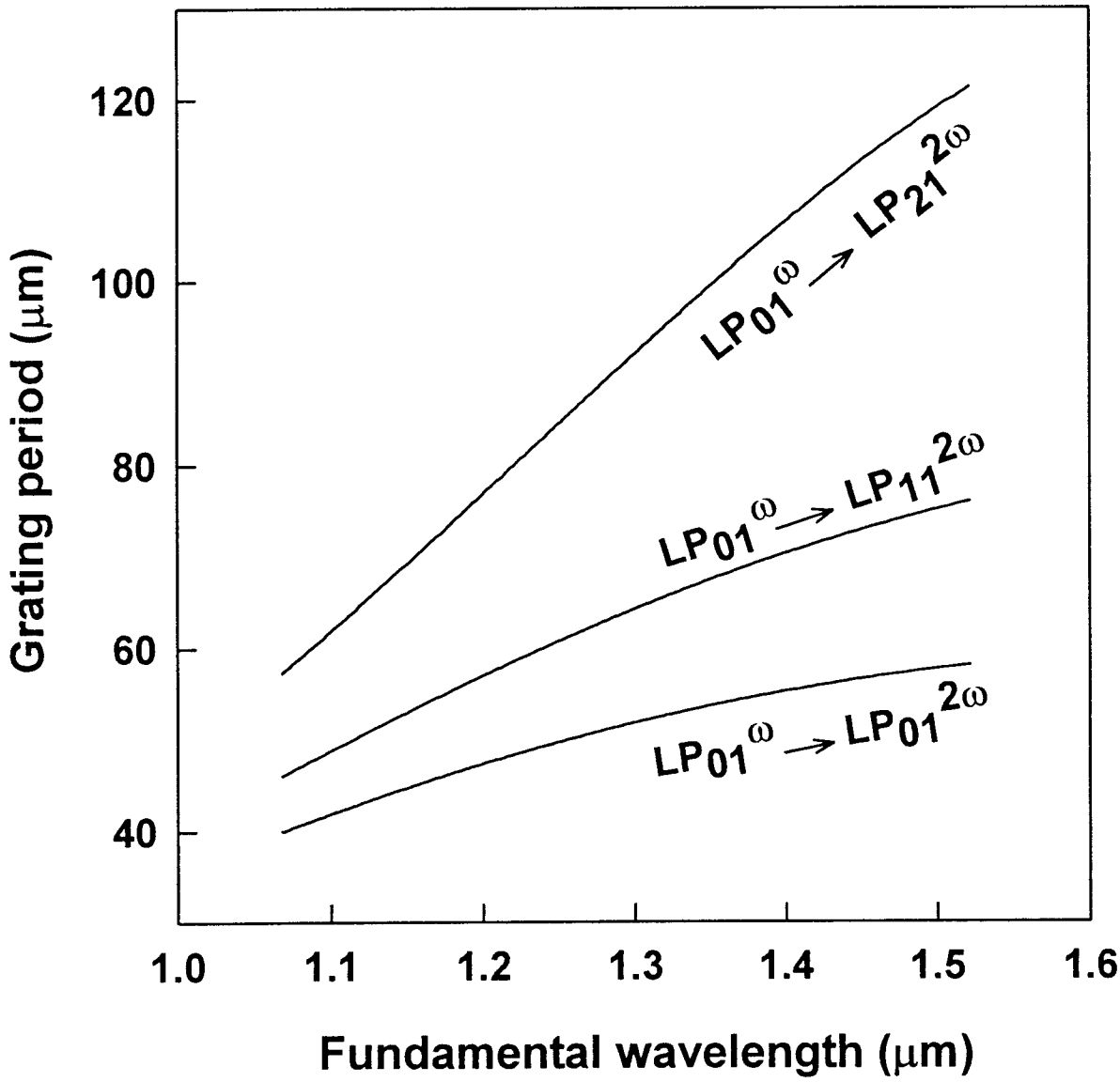

P.G. Kazansky and V. Pruneri "Electric field poling of quasi-phase-matched optical fibres", Fig.2b

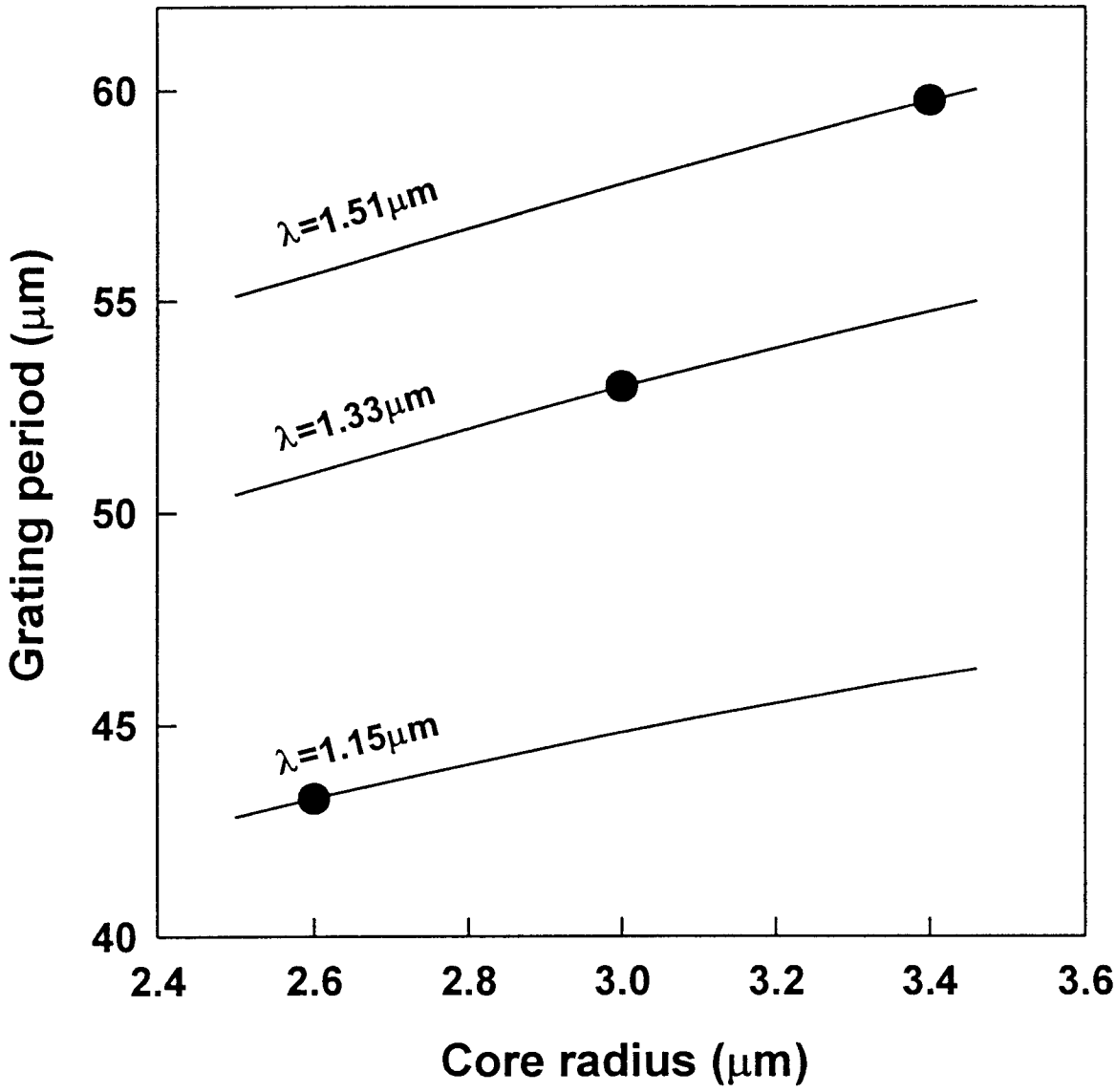

P.G. Kazansky and V. Pruneri "Electric field poling of quasi-phase-matched optical fibres", Fig.4

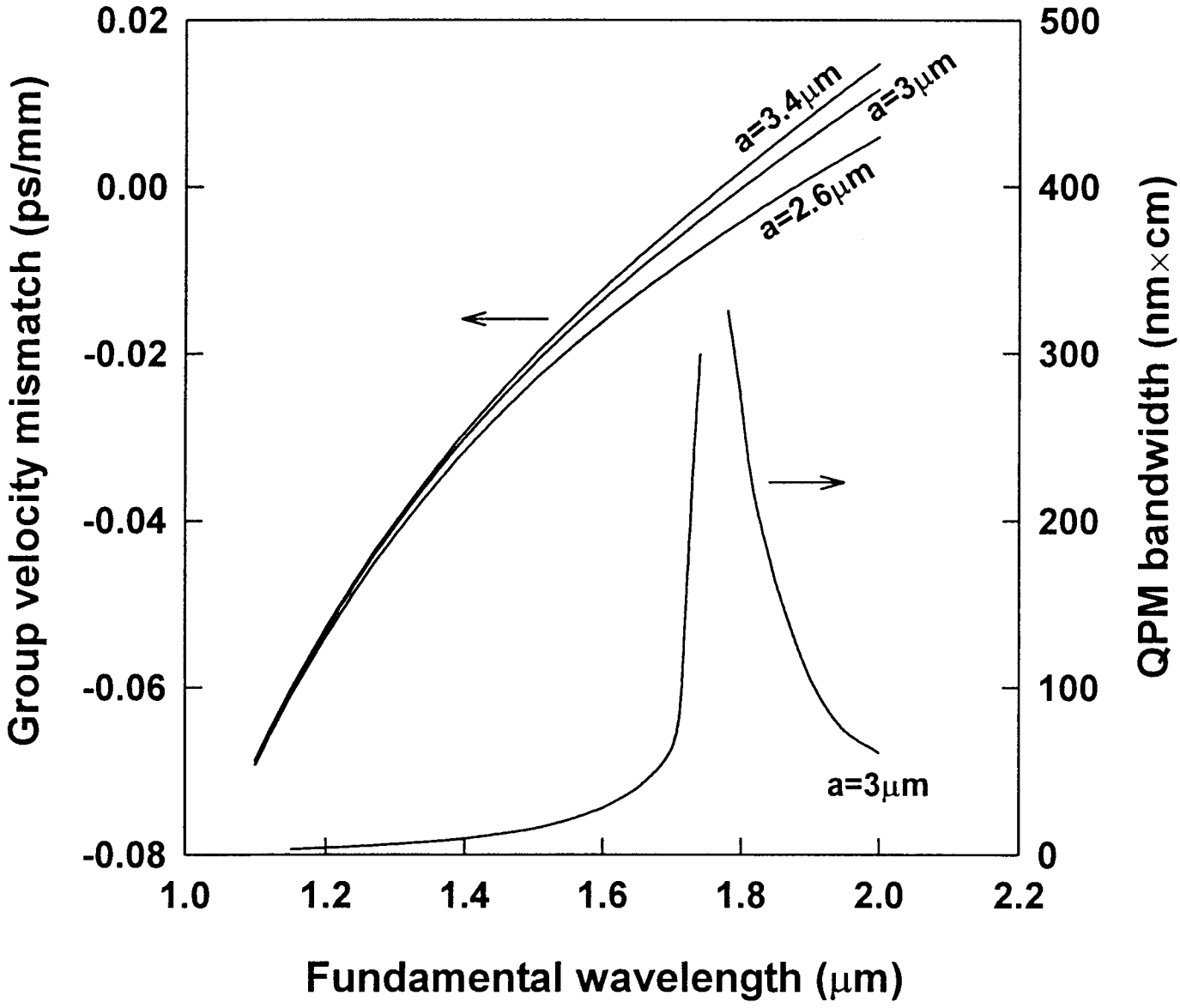

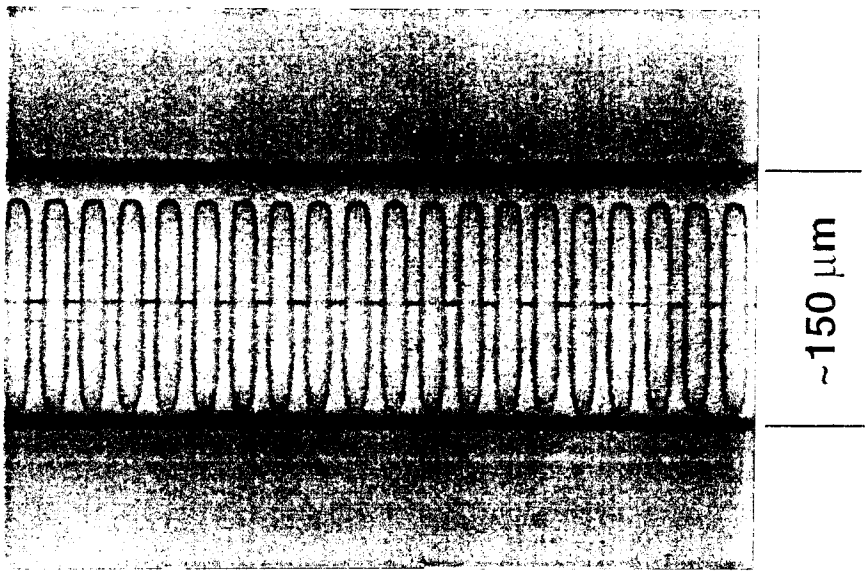
~150 μm

P.G. Kazansky and V. Pruneri "Electric field poling of quasi-phase-matched optical fibres", Fig.6

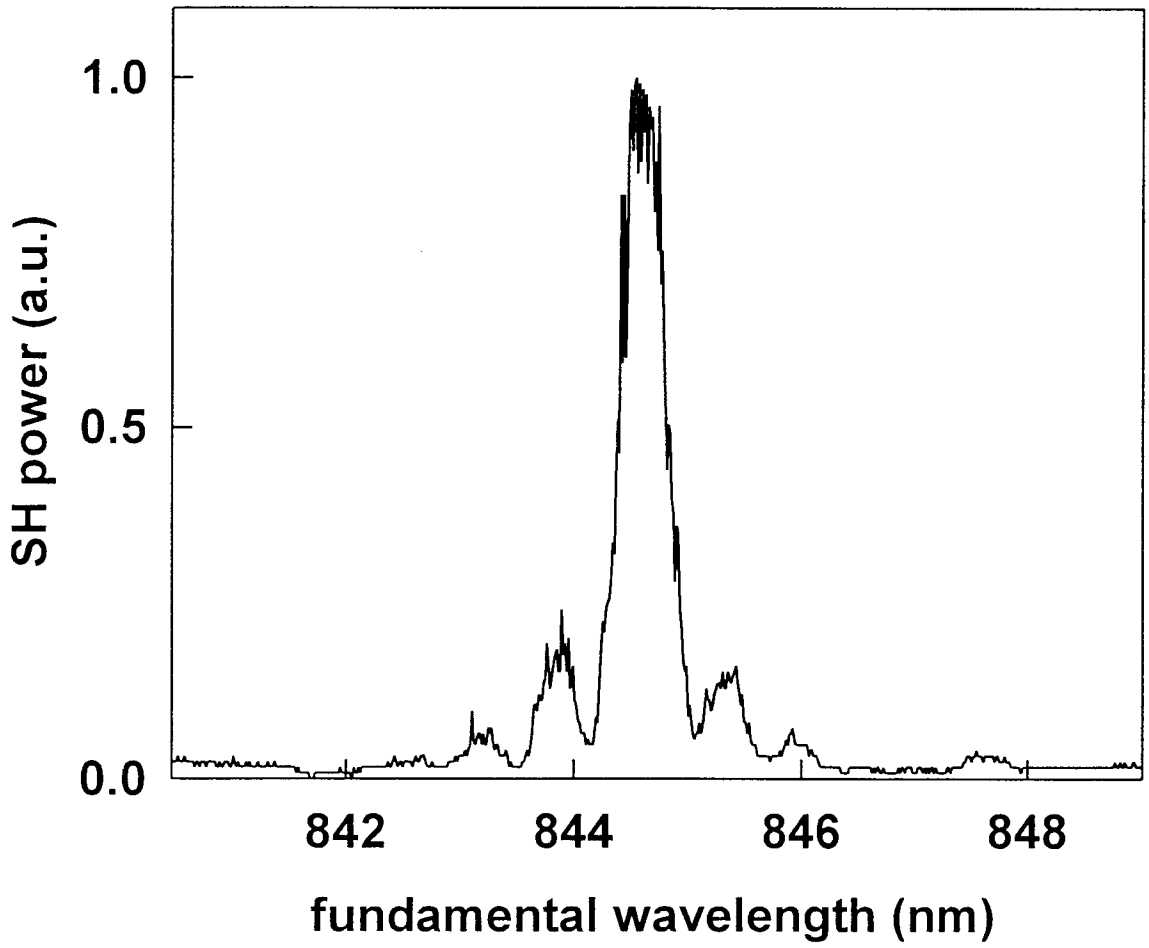

P.G. Kazansky and V. Pruneri "Electric field poling of quasi-phase-matched optical fibres", Fig.7

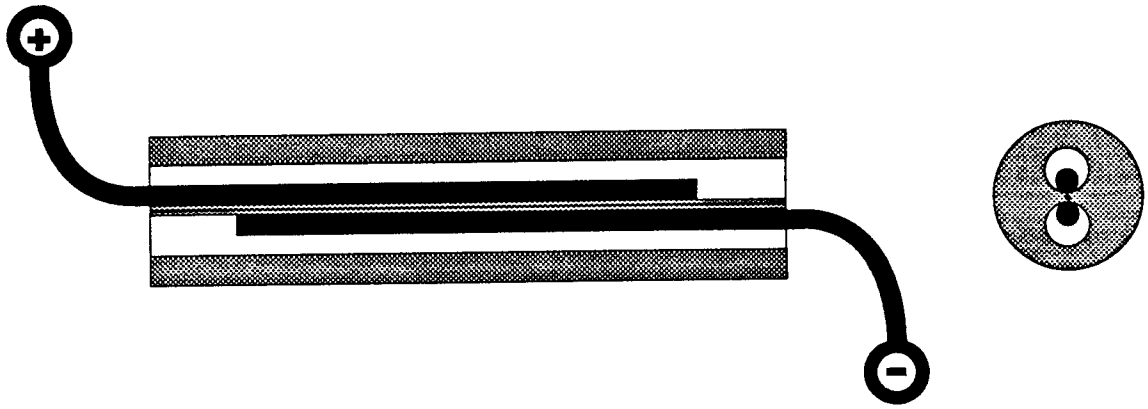

P.G. Kazansky and V. Pruneri "Electric field poling of quasi-phase-matched optical fibres", Fig.8

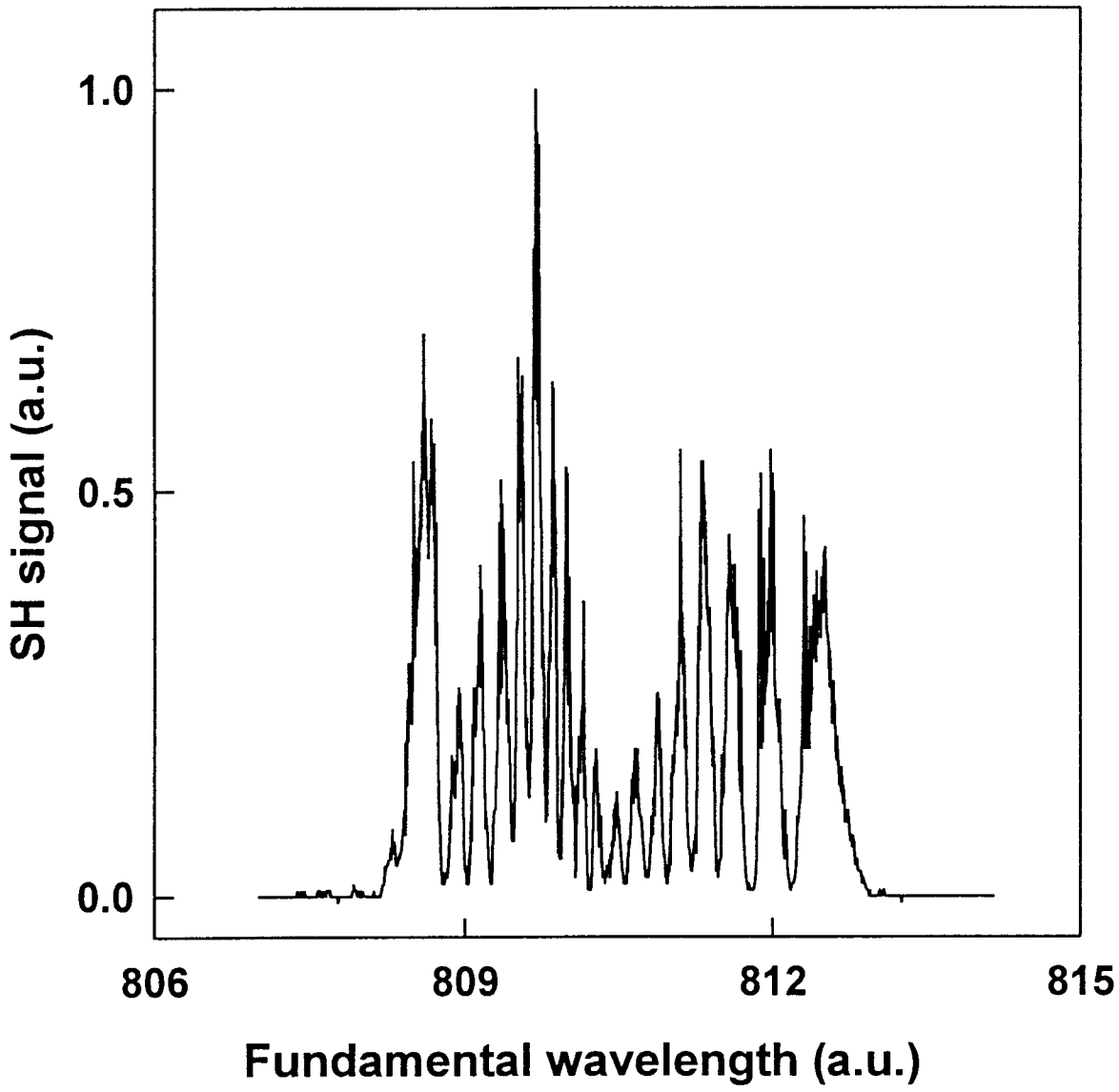

P.G. Kazansky and V. Pruneri "Electric field poling of quasi-phase-matched optical fibres", Fig.9

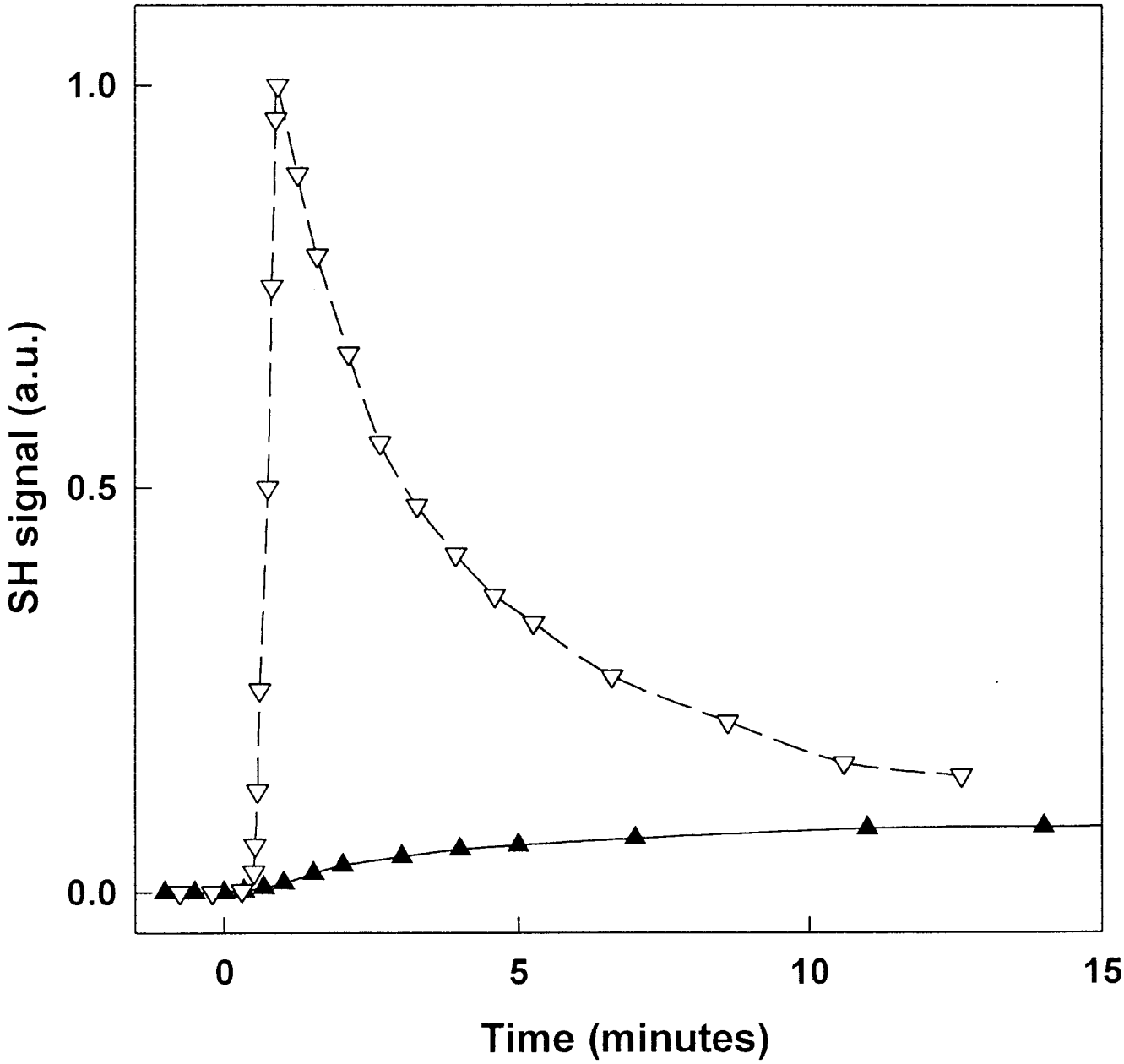

P.G. Kazansky and V. Pruneri "Electric field poling of quasi-phase-matched optical fibres", Fig.10

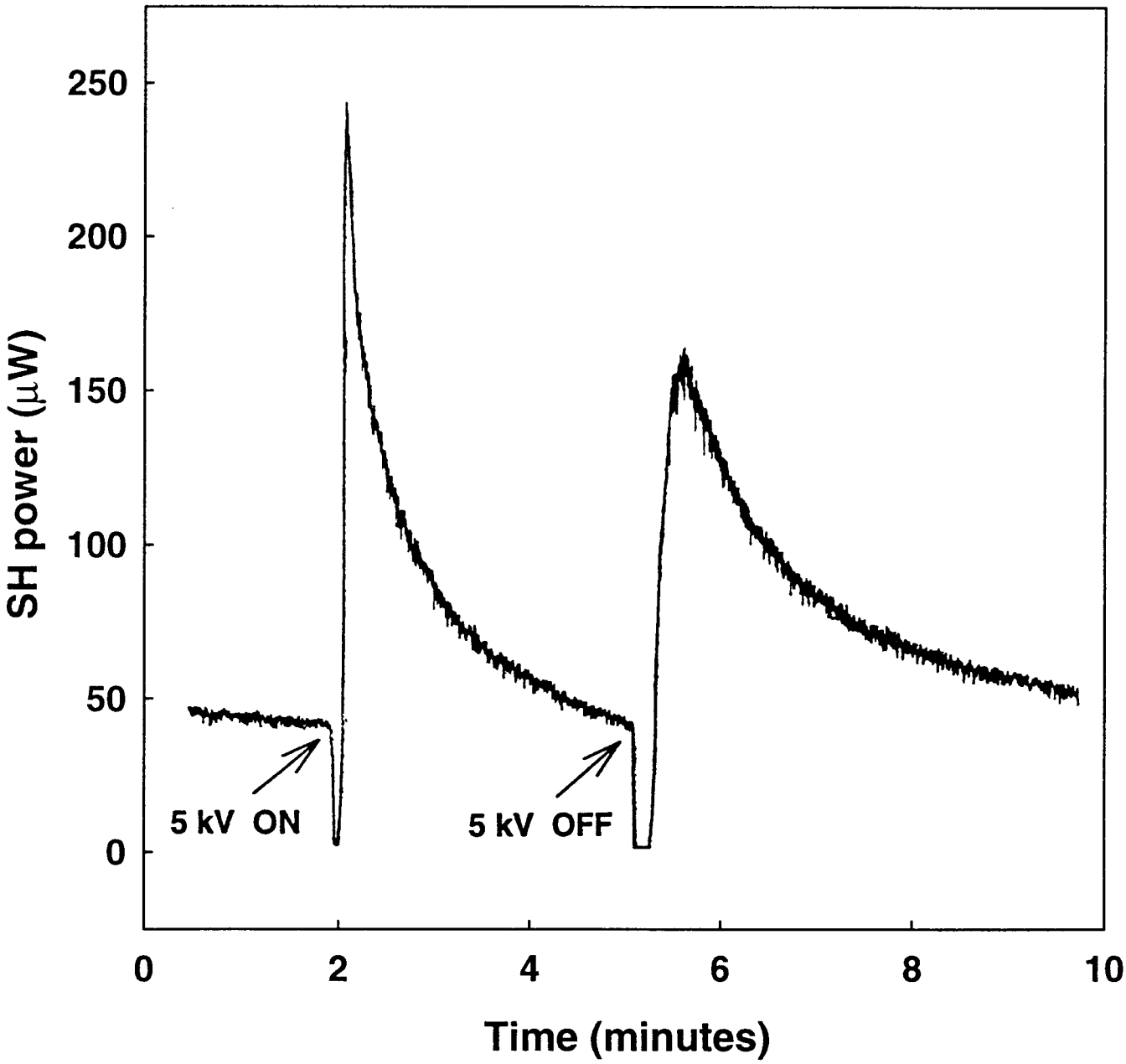

P.G. Kazansky and V. Pruneri "Electric field poling of quasi-phase-matched optical fibres", Fig.11a

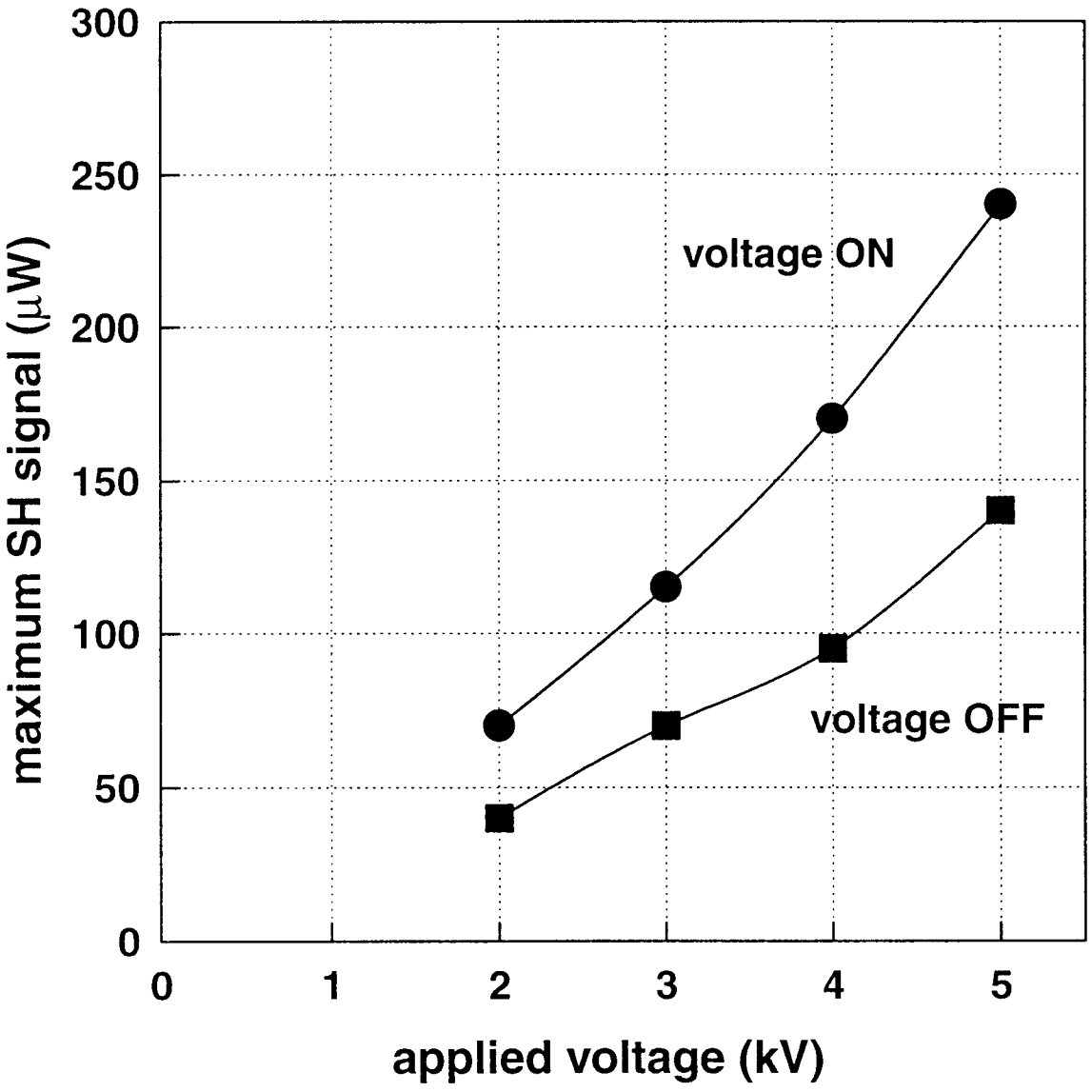

P.G. Kazansky and V. Pruneri "Electric field poling of quasi-phase-matched optical fibres", Fig.11b